CYCLIC BENDING RESPONSE AND FAILURE OF 6063-T5 ALUMINUM ALLOY OVAL SQUARE TUBES

[1]MIN-CHENG YU, [2]WEN-FUNG PAN

[1,2]Department of Engineering Science, National Cheng Kung University, 701 Tainan City, Taiwan
E-mail: [1]n98114023@gs.ncku.edu.tw, [2]z7808034@email.ncku.edu.tw

Abstract - This paper investigates the response and failure of 6063-T5 aluminum alloy oval square tubes with four different long/short axis ratios (1.5, 2.0, 2.5, and 3.0) under cyclic bending. The wall thickness is 0.7 mm for all oval square tubes, and cyclic bending loads are applied until fracture failure occurs. The experimental moment-curvature relationships exhibit stable loops for all long/short axis ratios. The experimental relationships between short axis variation and curvature (where short axis variation represents the change in the length of the short axis divided by the original length of the short axis) demonstrate symmetry, serrations, and a growth pattern as cycles progress. Moreover, a larger long/short axis ratio corresponds to a greater short axis variation. Regarding the curvature-number of cycles required to initiate fracture relationships, it can be observed that the four long/short axis ratios correspond to four straight lines when plotted on double logarithmic coordinates. Lastly, this study proposes theoretical equations to describe the aforementioned relationships. The theoretical analysis is compared with experimental data, revealing a close alignment between the two approaches. This indicates that the theory can reasonably describe the experimental results.

Keywords - 6063-T5 Aluminum Alloy Oval Square Tubes, Long/Short Axis Ratios, Moment, Curvature, Short Axis Variation, Cyclic Bending, Failure.

I. INTRODUCTION

Traditional circular tubes are commonly employed as pipes or support structures. However, they exhibit limitations in terms of load-bearing capacity, wear resistance, and shock absorption. In contrast, oval square tubes offer several advantages, including enhanced fluid dynamics, superior load-bearing capacity, heightened wear resistance, and increased shock absorption. By capitalizing on these benefits and combining them with the excellent properties of 6063-T5 aluminum alloy, such as corrosion resistance, high ductility, ease of processing, and strong tensile strength. 6063-T5 aluminum alloy oval square tubes (as depicted in Fig. 1) find extensive applications across various domains.

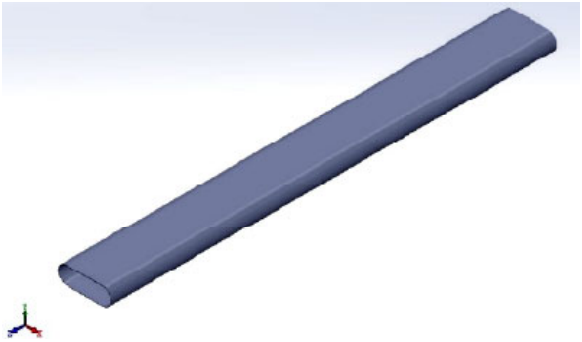


Fig. 1. Schematic diagram of an oval square tube.

Nonetheless, oval square tubes often encounter the challenge of enduring cyclic bending loads. These loads induce a gradual reduction in bending rigidity as the bending moment increases or as the number of cycles rises. This phenomenon is referred to as the degradation phenomenon, with the short axis variation serving as an apt descriptor of this behavior. Eventually, fracture failure transpires when the short axis variation surpasses a critical threshold.

So far, significant progress has been achieved in the study of bending behaviors exhibited by smooth circular tubes. In 1987, Kyriakides and Shaw [1] developed a mechanical apparatus capable of conducting monotonic or cyclic bending tests on circular tubes with or without external pressure. The materials investigated encompassed 1020 steel, 1018 steel, 304 stainless steel, 6061-T6 aluminum alloy, and NiTi circular smooth tubes [1-9]. Other researchers have similarly reported relevant findings. For instance, Yuan and Mirmiran [10] examined the buckling behavior of fiber-reinforced concrete-filled plastic pipes, Elchalakani et al. [11] ascertained the slenderness limit of cold-formed CHS (circular hollow sections) featuring fully ductile profiles by conducting cyclic bending tests at varying amplitudes. Houliara and Karamanos [12] explored the in-phase bending buckling response of tubes subject to external pressure, Yazdani and Nayebi [13] investigated the damage sustained by pipes undergoing periodic bending while under steady internal pressure, Elchalakani et al. [14] employed strains observed in bending tests to establish novel ductile slenderness limits for the plastic design of concrete-filled-tube structures, Shamass et al. [15] delved into the instability of circular tubes following non-proportional paths, Li and Wang [16] examined the instability of a single-layer cable-reinforced reticulated shell when subjected to seismic forces, and Chegeni et al. [17] explored the impact of corrosion depth and shape on the performance of curved pipes under specific internal pressure conditions. Silveira et al. [18] demonstrated the applicability of the constructal law in evaluating the

mechanical geometry of materials engineering systems. He et al. [19] proposed the relationship between the bending angle and the length of the transition section formation zone through experimental and simulation verification. Wang et al. [20] conducted a four-point bending experimental study on the bending response of square steel tube concrete reinforced by internal angle steel.

Pan et al. [21] developed a device in 1988, which enables the measurement of curvature and ovalization of circular tubes during bending. Their work involved a range of bending experiments on smooth circular tubes, including cyclic bending experiments [22], viscoplastic cyclic bending experiments [23], pure bending creep experiments [24], cyclic bending experiments with varying mean curvatures [25], and cyclic bending experiments with varying mean moments [26].

Starting from 2010, Pan et al. shifted their focus towards investigating the behavior of notched circular tubes under bending loads. For instance, they conducted cyclic bending tests on circular tubes featuring circumferential sharp notches [27-29], as well as cyclic bending tests on circular tubes incorporating localized sharp notches [30] and sharp dents [31]. Furthermore, Lee and colleagues conducted a series of studies on the response and failure of round-hole tubes [32-33] under cyclic bending.

Given the absence of pertinent research concerning the behavior of oval square tubes under bending loads, this paper aims to investigate the response and failure of 6063-T5 aluminum alloy oval square tubes under cyclic bending loads. The study encompasses four distinct long/short axis ratios: 1.5, 2.0, 2.5, and 3.0. To achieve this, cyclic bending tests were conducted using appropriate experimental apparatus. Various parameters, including the bending moment, curvature, short axis variation, and the number of cycles required to initiate fracture, were meticulously measured and analyzed.

II. DETAILS EXPERIMENTAL

2.1. Benging Device

In this study, a four-point bending machine was utilized to conduct cyclic bending tests on 6063-T5 aluminum alloy oval square tubes, as depicted in Fig. 2. The setup comprises two rotating sprockets positioned on two supporting beams. A robust chain runs around these sprockets, which are supported by heavy-duty beams. This configuration allows for test specimens with a maximum length of 1 meter. To facilitate the testing, each tube is outfitted with solid rod extensions, as illustrated in Fig. 3. Throughout the bending process, the interaction between the tube and the roller permits free axial movement. The load applied to the test specimen is generated by means of two concentrated loads originating from a pair of rollers. Upon retraction of the upper or lower cylinder, the sprocket initiates rotation, facilitating pure bending of the test specimen. To achieve reverse bending, the hydraulic circuit's flow direction is reversed.

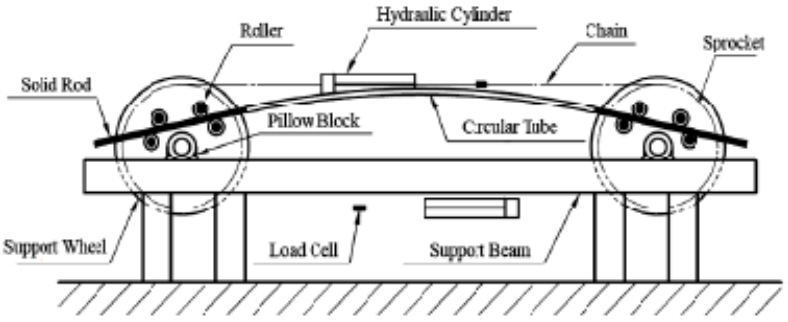


Fig. 2. Schematic diagram of the tube-bending machine.

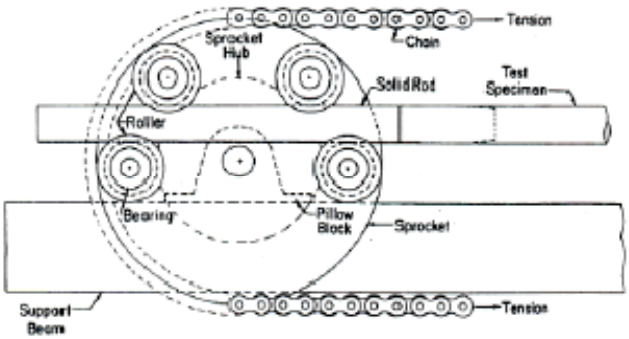


Fig. 3. Enlarged schematic diagram of the sprocket.

Nonetheless, the spatial confines of the rollers can only accommodate the insertion of solid rods with circular cross-sections, as depicted in Fig. 3. Inserting a solid rod with a circular cross-section into the oval square tube proves unfeasible. To address this challenge, this study undertakes necessary adaptations to the solid rod design. As illustrated in Fig. 4, a new solid rod configuration is devised for use with the tube-bending machine. This figure shows that the newly devised solid rod combines an oval square cross-section on one end and a circular cross-section on the other. The fusion of these components is achieved through welding on both contact surfaces, resulting in the creation of the novel solid rod. Given that this investigation involves four distinct long/short axis ratios, the oval square cross-section solid rods on one end must be of varying sizes—four sizes, to be precise. Conversely, the circular cross-section solid rods on the other end maintain a consistent size, as shown in Fig. 5.



Fig. 4. A novel solid rod.



Fig. 5. Four solid rods for four distinct long/short axis ratios.

2.2. Curvature-Ovalization Measurement Apparatus (COMA)

The COMA devised by Pan et al. [21], illustrated in Fig. 6, serves as a tool for gauging tube curvature and the cross-sectional ovalization of tubes. Ovalization is defined as the alteration of the outer diameter divided by the original outer diameter. This lightweight instrument is conveniently situated in proximity to the mid-span of the tube. Leveraging the fixed spacing between the two side-inclinometers and the angular shifts identified by these inclinometers, tube curvature can be easily computed. Furthermore, the COMA incorporates a magnetic detector positioned at its center to assess alterations in the outer diameter, enabling the determination of round tube ovalization. In this particular study, the COMA was employed to track variations in the short axis of the oval square tube, thereby facilitating the acquisition of short axis changes. A comprehensive exposition of the COMA can be found in the work by Pan et al. [21].

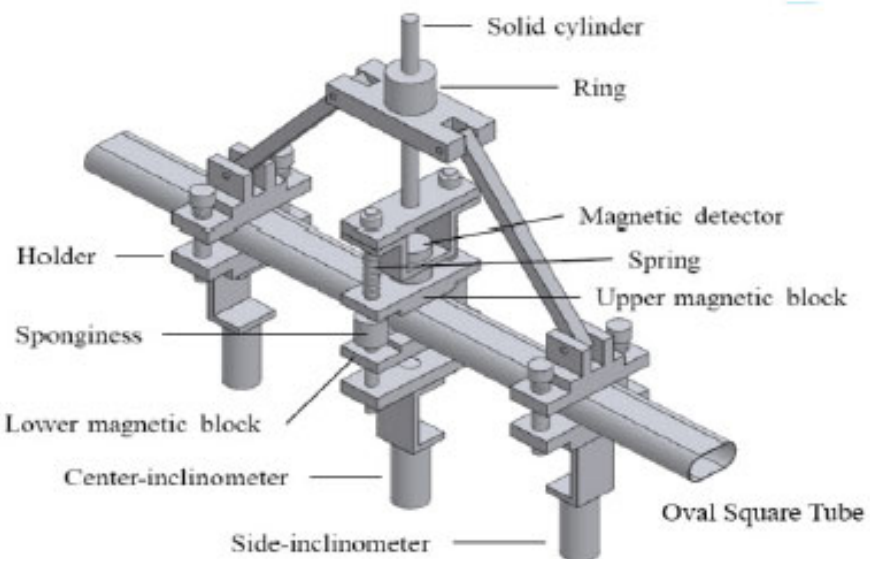


Fig. 6. Schematic diagram of the COMA.

2.3. 6063-T5 Aluminum Alloy Oval Square Tubes

The experiment utilized the 6063-T5 aluminum alloy oval square tubes, and Tables 1 and 2 respectively show the chemical composition and mechanical properties of the 6063-T5 aluminum alloy. The length of the oval square tubes is 500 mm, with a thickness of 0.7 mm. Fig. 7 shows the schematic diagram of the long axis and short axis of the cross-section of an oval square tube. In this study, four different long/short axis ratios (ℓlong/ℓshort ratios), 1.5 (30mm/20mm), 2.0 (40mm/20mm), 2.5 (50mm/20mm), and 3.0 (60mm/20mm) were considered as shown in Fig. 8.

Element	Al	Cr	Cu	Mn	Si	Ti	Zn	Mg	Fe
Proportion (%)	97	0.10	0.10	0.10	0.20	0.10	0.10	0.45	0.35

Table 1. Chemical composition of the 6063-T5 aluminum alloy (weight %)

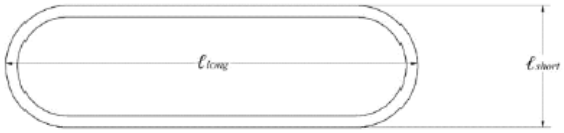


Fig. 7. Schematic diagram illustrating the long axis and short axis of the cross-section of an oval square tube.

Density	2.70 g/cm^3
Young's Modulus	68.9 GPa
Poisson's Ratio	0.33
Yield Strength	145 MPa
Ultimate Strength	186 MPa

Table 2. Mechanical properties of the 6063-T5 aluminum alloy.



Fig. 8. 6063-T5 aluminum alloy oval square tubes with four different ℓlong/ℓshort ratios.

2.4. Test Procedures

The experiment entailed a curvature-controlled cyclic bending test, characterized by a curvature rate of 0.05 m-1s-1. In this investigation, the direction of the bending moment coincided with the long axis direction, specifically the x-direction, as shown in the 3D Fig. 1. This bending load condition is common to most oval square tubes. The controlled-curvature ranges spanned from -0.5 m-1 to +0.5 m-1, and extended further to -0.8 m-1 to +0.8 m-1. The bending moment (M) was ascertained through load cells incorporated into the bending machine, as depicted in Fig. 2. The curvature (κ) and short axis variation (Δℓ/ℓshort, where Δℓ is the change in ℓshort) were measured by the apparatus in Fig. 6. Simultaneously, the number of cycles required to initiate fracture (Nf) was recorded.

III. RESULTS AND DISCUSSION

3.1. Moment (M)-Curvature (κ) Relationships

Figs. 9(a)-(d) respectively present the experimental M-κ relationships of 6063-T5 aluminum alloy oval square tubes with ℓ_{long}/ℓ_{short} ratios of 1.5, 2.0, 2.5, and 3.0 under cyclic bending. The κ was controlled within the range of +0.5 m-1 to -0.5 m-1. During the initial loading stage, the oval square tube remains within the elastic range, resulting in a linear growth in the M-κ relationship. As κ increases, the oval square tube begins to deform plastically, leading to a gradual flattening of the M-κ relationship and causing permanent deformation. The experimental results also show that all M-κ curves stabilize in the first cycle or within a few cycles. Additionally, under the same κ, as the ℓ_{long}/ℓ_{short} ratio increases, the peak value of M increases. For instance, when ℓlong/ℓshort ratio is 1.5, the peak M value is ±51 N-m; while for an ℓ_{long}/ℓ_{short} ratio of 3.0, the peak M value increases to ±83 N-m. Notably, different κ values exhibit similar phenomena. Therefore, this study only presents the M-κ relationship for κ = ±0.5 m-1 and ℓ_{long}/ℓ_{short} ratios of 1.5, 2.0, 2.5, and 3.0.

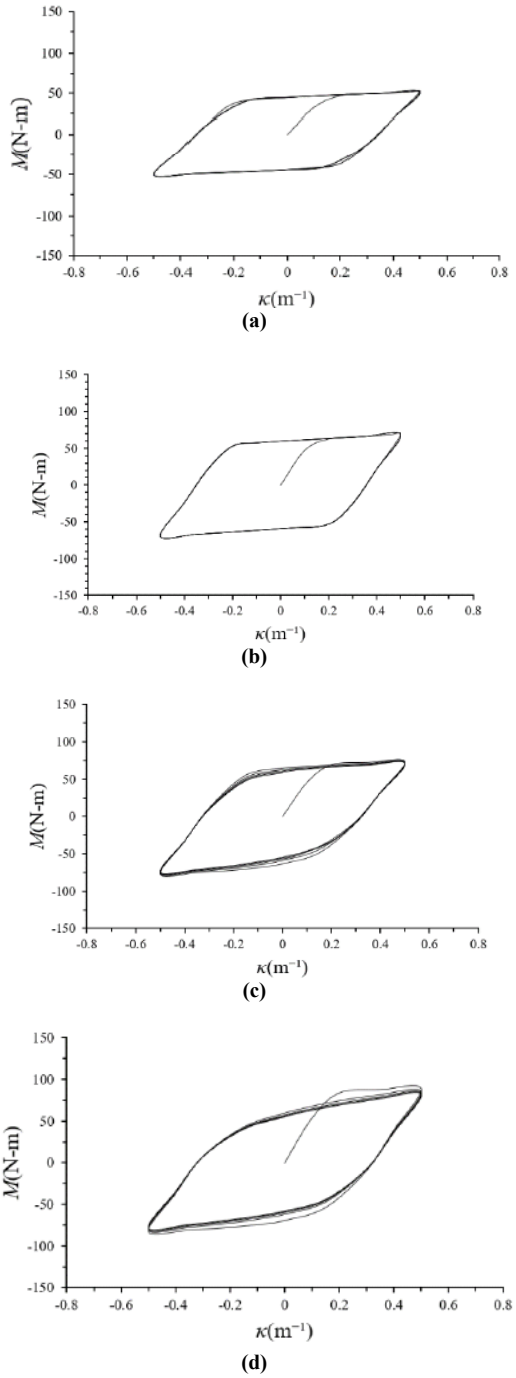
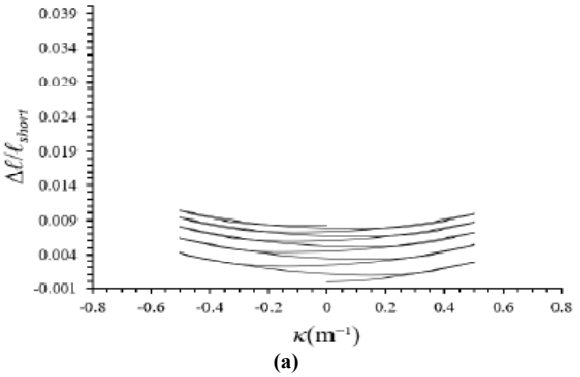


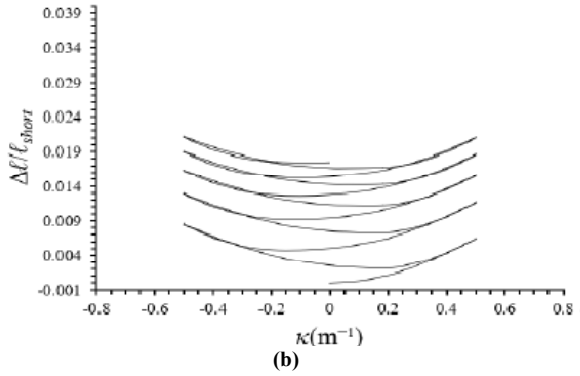
Fig. 9. Experimental M-κ relationships of 6063-T5 aluminum alloy oval square tubes with ℓlong/ℓshort ratios of (a) 1.5, (b) 2.0, (c) 2.5, and (d) 3.0 under cyclic bending.

3.2. Short Axis Variation (Δℓ/ℓshort)-Curvature (κ) Relationships

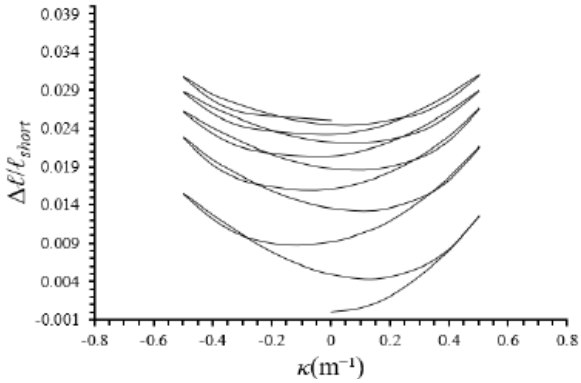
Figs. 10(a)-(d) showcase the experimental Δℓ/ℓshort-κ relationships of 6063-T5 aluminum alloy oval square tubes with ℓlong/ℓshort ratios of 1.5, 2.0, 2.5, and 3.0 under cyclic bending. The κ values were similarly confined within the range of +0.5 m-1 to -0.5 m-1. Evidently, the Δℓ/ℓshort-κ relationship follows a pattern marked by symmetry, ratcheting, and incremental growth as the cycling progresses. Under the same κ value, a higher ℓlong/ℓshort ratio corresponds to a more pronounced Δℓ/ℓshort. Notably, different κ values exhibit similar phenomena. Therefore, this study only depicts the Δℓ/ℓshort-κ relationship for κ = ±0.5 m-1 and ℓlong/ℓshort ratios of 1.5, 2.0, 2.5, and 3.0.



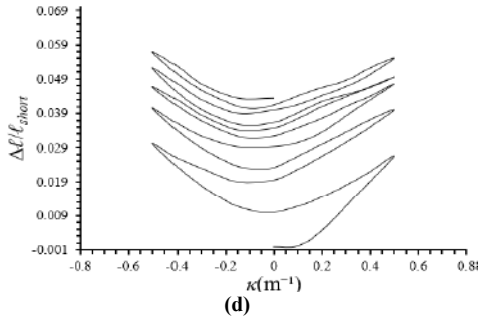
(a)



(b)



(c)



(d)

Fig. 10. Experimental Δℓ/ℓshort-κ relationships of 6063-T5 aluminum alloy oval square tubes with ℓlong/ℓshort ratios of (a) 1.5, (b) 2.0, (c) 2.5, and (d) 3.0 under cyclic bending.

3.3. Control Curvature(κ_c)-Number of CyclesRequired to Initiate Fracture (Nf) Relationships

Fig. 11 presents the experimental κc-Nf relationships of 6063-T5 aluminum alloy oval square tubes with four different ℓlong/ℓshort ratios under cyclic bending. Notably, as observed from the Fig. 11, when maintaining a constant ℓlong/ℓshort ratio, Nf diminishes with an increase in κc. Similarly, for a consistent κc, Nf experiences a decline as the ℓlong/ℓshort ratio increases. In Fig. 12, the same data shown in Fig. 11 are depicted on a double logarithmic scale. The straight lines featured on the plot are the results of the least squares method. Upon examining the plot, it becomes evident that the four distinct ℓlong/ℓshort ratios correspond to four straight lines.

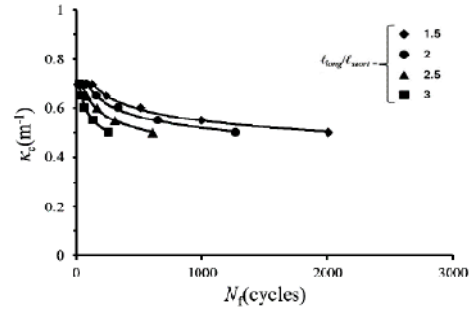


Fig. 11. Experimental κc-Nf relationships of 6063-T5 aluminum alloy oval square tubes with four different ℓlong/ℓshort ratios under cyclic bending.

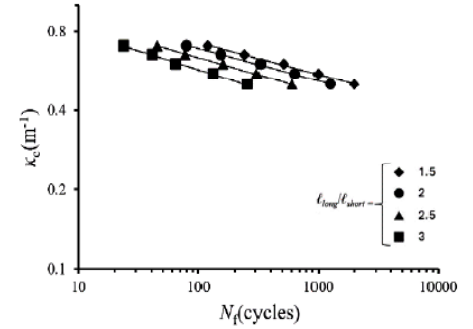


Fig. 12. Experimental κc-Nf relationships of 6063-T5 aluminum alloy oval square tubes with four different ℓlong/ℓshort ratios under cyclic bending on double logarithmic coordinates.

3.2. Theoretical Analysis

In 1987, Kyriakides and Shaw [1] proposed the κ_c/κ_o-N_b (number of cycles required to initiate buckling) relationship for smooth circular tubes under cyclic bending loads to be:

$$\kappa_c/\kappa_o = C(N_b)^{-\alpha} \quad (1)$$

or

$$\log\kappa_c/\kappa_o = \log C - \alpha \log N_b, \quad (2)$$

where κ_o is utilized to represent the dimensionless parameter κ, which is defined as the tube thickness divided by the square of the outer diameter, while C and α are material parameters. C signifies the value of κ_c/κ_o when N_b equals 1, and α denotes the slope of the straight line in the κ_c/κ_o-N_b relationship on double logarithmic coordinates. Since the current experiment employs oval square tubes, determining κ_o becomes infeasible. Consequently, Eq. (1) is expressed as follows:

$$\kappa_c = C(N_f)^{-\alpha} \quad (3)$$

or

$$\log\kappa_c = \log C - \alpha \log N_f, \quad (4)$$

Based on the experimental data, the relationships between C and ℓ_{long}/ℓ_{short} ratios are fitted and depicts in Fig. 13. The straight line in the plot was obtained through the least squares regression fitting method. The linear trends observed in these relationships enable the formulation of the following expression:

$$C = c_1(\ell_{long}/\ell_{short}) + c_2 \quad (5)$$

where c_1 and c_2 are material parameters, which can be obtained from the fitting of the relationships between C and ℓ_{long}/ℓ_{short} ratios as shown in Fig. 13. The specific material parameters are calculated to be c_1 = -0.0997 and c_2 = 1.3925.

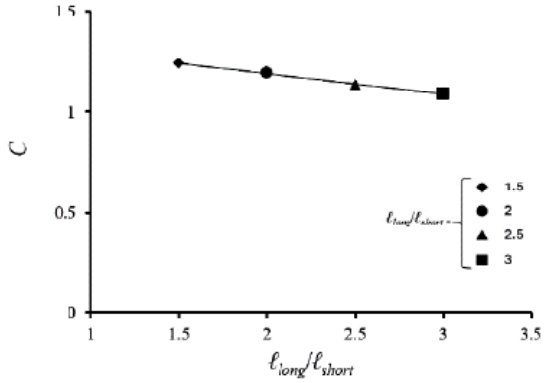


Fig. 13. Relationship between C and ℓlong/ℓshort ratios.

Based on the experimental data, the relationships between α and ℓlong/ℓshort ratios was fitted and depicts in Fig. 14. The straight line in the plot was obtained through the least squares regression fitting method. The linear trends observed in these relationships enable the formulation of the following expressions:

$$\alpha = a_1(\ell_{long}/\ell_{short}) + a_2, \quad (6)$$

where a1 and a2 are material parameters, which can be obtained from the fitting of the relationships between α and ℓ_{long}/ℓ_{short} ratios as shown in Fig. 14. The specific material parameters are calculated to be a1 = 0.0132 and a2 = 0.0978. Conclusively, Eqs. (3), (5), and (6) were employed to characterize the κc-Nf relationships of 6063-T5 aluminum alloy oval square tubes with different ℓ_{long}/ℓ_{short} ratios under cyclic bending. The outcomes of theoretical analysis are Cyclic Bending Response and Failure of 6063-T5 Aluminum Alloy Oval Square Tubes demonstrated as dashed lines in Fig. 15. Through comparison with the experimental results, it is evident that that the formulations introduced in this study adequately and reasonably describe the experimental findings.

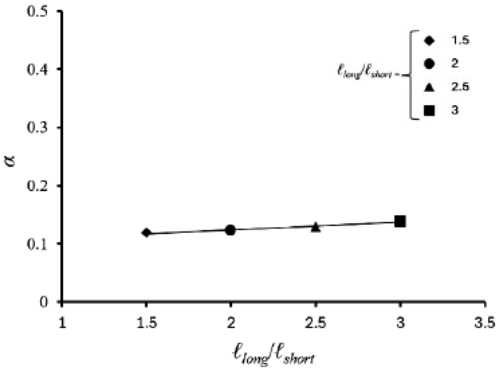


Fig. 14. Relationship α and ℓ_{long}/ℓ_{short} ratios

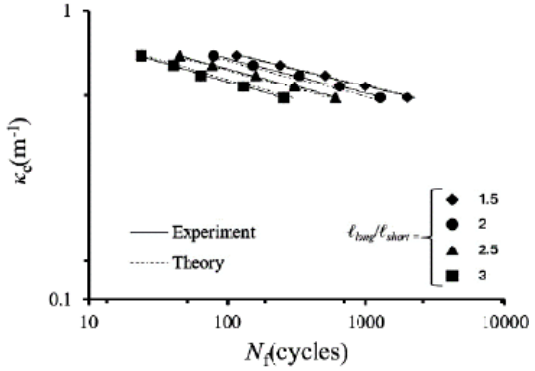


Fig. 15. Experimental and theoretical κc-Nf relationships of 6063-T5 aluminum alloy oval square tubes with different ℓlong/ℓshort ratios under cyclic bending on double logarithmic coordinates.

IV. CONCLUSION

This study delves into the behavior and failure mechanisms of 6063-T5 aluminum alloy oval square tubes with four different ℓ_{long}/ℓ_{short} ratios of 1.5, 2.0, 2.5, and 3.0 under cyclic bending. Based on both experimental findings and theoretical analyses, several key conclusions can be drawn from this research:

1. For the experimental M-κ relationships, different ℓ_{long}/ℓ_{short} ratios show stable elastic-plastic loops in the first cycle or after several cycles. Notably,

with consistent κ loading, an increasing in the ℓlong/ℓshort ratio leads to a higher peak M value.

2. For the experimental $\Delta\ell/\ell_{short}$-κ relationships, the data exhibit symmetry, serrations, and a growth pattern as cycles progress. Additionally, under the same κ loading condition, a larger ℓ_{long}/ℓ_{short} ratio results in a greater $\Delta\ell/\ell_{short}$.
3. For the experimental κc-Nf relationships, it is revealed that, while holding the ℓ_{long}/ℓ_{short} ratio constant, Nf decreases as κc increases. Similarly, at a fixed κc, Nf declines with higher ℓ_{long}/ℓ_{short} ratio. When considering the κc-Nf relationships on a log-log scale, it becomes evident that the four distinct ℓ_{long}/ℓ_{short} ratios correspond to four straight lines.
4. To describe the κc-Nf relationships, Eq. (3) was introduced. Using experimental data, Eqs. (5) and (6) were derived. Ultimately, Eqs. (3), (5), and (6) were employed to characterize the κc-Nf relationships for 6063-T5 aluminum alloy oval square tubes with different ℓlong/ℓshort ratios under cyclic bending. The theoretical calculations closely matched the experimental data, as illustrated in Fig. 15.

ACKNOWLEDGMENTS

The research was conducted with the generous support of the National Science and Technology Council, through grant MOST 112-2221-E-006-174. We extend our heartfelt gratitude for their invaluable assistance.

REFERENCES

[1] S. Kyriakides, and P.K. Shaw, “Inelastic buckling of tubes under cyclic loads”, ASME Journal of Pressure Vessels and Technology, vol. 109, no. 2, pp. 169-178,1987.

[2] E. Corona, and S. Kyriakides, “An experimental investigation of the degradation and buckling of circular tubes under cyclic bending and external pressure”, Thin-Walled Structures, vol. 12, no. 3, pp. 229-263, 1991.

[3] E. Corona, and S. Kyriakides, “Asymmetric collapse modes of pipes under combined bending and pressure”, International Journal of Solids and Structures, vol. 24, no. 5, pp. 505-535, 2000.

[4] E. Corona, L.H. Lee, and S. Kyriakides, “Yield anisotropic effects on buckling of circular tubes under bending”, International Journal of Solids and Structures, vol. 43, no. 22, pp. 7099-7118, 2006.

[5] A. Limam, L.H. Lee, E. Corona, and S. Kyriakides, “Inelastic wrinkling and collapse of tubes under combined bending and internal pressure”, International Journal of Mechanical Sciences, vol. 52, no. 5, pp. 37-47, 2010.

[6] A. Limam, L.H. Lee, and S. Kyriakides, “On the collapse of dented tubes under combined bending and internal pressure”, International Journal of Solids and Structures, vol. 55, no. 1, pp. 1-12, 2012.

[7] N. J. Bechle, and S. Kyriakides, “Localization of NiTi tubes under bending”, International Journal of Solids and Structures, vol. 51, no. 5, pp. 967-980, 2014.

[8] D. Jiang, S. Kyriakides, N.J. Bechle, and C.M. Landis, “Bending of pseudoelastic NiTi tubes”, International Journal of Solids and Structures, vol. 124, pp. 192-214, 2017.

[9] K. Kazinakis, S. Kyriakides, D. Jiang, N.J. Bechle, and C.M. Landis, “Buckling and collapse of pseudoelastic NiTi tubes under bending”, International Journal of Solids and Structures, vol. 221, pp. 2-17, 2021.

[10] W. Yuan, and A. Mirmiran, “Buckling analysis of concrete-filled FRP tubes”, International Journal of Structural Stability and Dynamics, vol. 1, no. 3, pp. 367-383, 2001.

[11] M. Elchalakani, X.L. Zhao, and R.H. Grzebieta, “Plastic mechanism analysis of circular tubes under pure bending”, International Journal of Mechanical Sciences, vol. 44, no. 6, pp. 1117-1143, 2002.

[12] S. Houliara, and S.A. Karamanos, “Buckling and post-buckling of long pressurized elastic thin-walled tubes under in-plane bending”, International Journal of Nonlinear Mechanics, vol. 41, no. 4, pp. 491-511, 2006.

[13] H. Yazdani, and A. Nayebi, “Continuum damage mechanics analysis of thin-walled tube under cyclic bending and internal constant pressure”, International Journal of Applied Mechanics, vol. 5, no. 4, 1350038 [20 pages], 2013.

[14] M. Elchalakani, A. Karrech, M.F. Hassanein, and B. Yang, “Plastic and yield slenderness limits for circular concrete filled tubes subjected to static pure bending”, Thin-Walled Structures, vol. 109, pp. 50-64, 2016.

[15] R. Shamass, G. Alfano, and F. Guarracino, “On elastoplastic buckling analysis of cylinders under nonproportional loading by differential quadrature method”, International Journal of Structural Stability and Dynamics, vol. 17, no. 7, 1750072 [40 pages], 2017.

[16] P. Li, and L. Wang, “Nonlinear stability behavior of cable-stiffened single-layer latticed shells under earthquakes”, International Journal of Structural Stability and Dynamics, vol. 18, no. 10, 1850117 [24 pages], 2018.

[17] B. Chegeni, S. Jayasuriya, and S. Das, “Effect of corrosion on thin-walled pipes under combined internal pressure and bending”, Thin-Walled Structures, vol. 143, 106218 [8 pages], 2019.

[18] T. Silveira1, V.T. Pinto, J.P.S. Neufeld, A. Pavlovic, L.A.O. Rocha, E.D. Santos, and L.A. Isoldi, “Applicability evidence of constructal design in structural engineering: Case study of biaxial elasto-plastic buckling of square steel plates with elliptical cutout”, Journal of Applied and Computational Mechanics, vol. 7, no. 2 pp. 922-934, 2021.

[19] Z.R. He, G.J. Li, J.C. Yang, X.Z. Guo, X.Y. Duan, W. Guo, X. Liu, Y.Y. Deng, and C. Cheng, “Insight into the deformation transition effect in free bending of tubes”, Materials Letters, vol. 348, 134673, 2023.

[20] J. Wang, J.R. Li, H. Li, and L.Y. Lv, “Behaviour of square concrete-filled steel tubes reinforced with internal latticed steel angles under bending”, Structures, vol. 48, pp. 1436-1454, 2023.

[21] W.F. Pan, T.R. Wang, and C.M. Hsu, “A curvature-ovalization measurement apparatus for circular tubes under cyclic bending”, Experimental Mechanics, vol. 38, no. 2, pp. 99-102, 1998.

[22] K.L. Lee, W.F. Pan, and J.N. Kuo, “The influence of the diameter-to-thickness ratio on the stability of circular tubes under cyclic bending”, International Journal of Solids and Structures, vol. 38, no. 14, pp. 2401-2413, 2001.

[23] W.F. Pan, and Y.S. Her, “Viscoplastic collapse of thin-walled tubes under cyclic bending”, ASME Journal of Engineering Materials and Technology, vol. 120, no. 4, pp. 287-290, 1998.

[24] W.F. Pan, and K.L. Lee, “Pure bending creep of SUS304 stainless steel tubes”, Steel and Composite Structures, vol. 2, no. 6, pp. 461-474, 2002.

[25] W.F. Pan, and K.L. Lee, “The effect of mean curvature on the response and collapse of thin-walled tubes under cyclic bending”, JSME International Journal, Series A, vol. 28, no. 2, pp. 495-514, 2002.

[26] K.H. Chang, W.F. Pan, and K.L. Lee, “Mean moment effect of thin-walled tubes under cyclic bending”, Structural Engineering and Mechanics, vol. 28, no. 5, pp. 505-535, 2008.

[27] K.L. Lee, “Mechanical behavior and buckling failure of sharp-notched circular tubes under cyclic bending”, Structural Engineering and Mechanics, vol. 34, no. 3, pp. 367-376, 2010.

[28] K.L. Lee, C.M. Hsu, and W.F. Pan, "Viscoplastic collapse of sharp-notched circular tubes under cyclic bending", Acta Mechanica Solida Sinica, vol. 26, no. 6, pp. 629-641, 2013.
[29] K.L. Lee, C.C. Chung, and W.F. Pan, "Growing and critical ovalization for sharp-notched 6061-T6 aluminum alloy tubes under cyclic bending", Journal of the Chinese Institute of Engineers, vol. 39, no. 8, pp. 926-935, 2016.
[30] K.L. Lee, K.H. Chang, and W.F. Pan, "Effects of notch depth and direction on stability of local sharp-notched circular tubes
[31] subjected to cyclic bending", International Journal of Structural Stability and Dynamics, vol. 18, no. 7, 1850099 [23 pages], 2018.
[32] K.L. Lee, C.C. Chung, and W.F. Pan, "Cyclic bending deterioration and failure of locally-dented circular tubes", Journal of the Chinese Society of Mechanical Engineers, vol. 39, no. 1, pp. 53-63, 2018.
[33] K.L. Lee, H.Y. Liu, and W.F. Pan, Response of round-hole tubes submitted to pure bending creep and pure bending relaxation, Advances in Mechanical Engineering, vol. 13, no. 9., pp. 1-17, 2021.
[34] K.L. Lee, Y.C. Chou, and W.F. Pan, "Ovalization growth and critical ovalization of round-hole tubes with different hole diameters and hole directions subjected to cyclic bending", Informatica Journal, vol. 34, no. 4, pp. 139-157, 2023.

★★★